Supporting Information

Antibacterial Activity of Two-Dimensional MoS_2 Sheets

Xi Yang, Jie Li, Tao Liang, Chunyan Ma, Yingying Zhang, Hongzheng Chen, Nobutaka Hanagata,* Huanxing Su,* and Mingsheng Xu**

1. Superoxide radical anion production by MoS_2 materials

The possibility of superoxide radical anion ($O_2^{\bullet-}$) production was evaluated by monitoring the absorption of XTT (2, 3-bis (2-methoxy-4-nitro-5-sulfophenyl)-2H-tetrazolium-5-carboxanilide, Fluka). XTT can be reduced by superoxide radical anion ($O_2^{\bullet-}$) to form water-soluble XTT-formazan with the maximum absorption at 470 nm.

XTT (0.4 mM) was dissolved in phosphate buffered saline (PBS) solution at pH 7.0. dispersions of MoS_2 materials (80 μg/mL, 1 mL) in a PBS buffer (80 μg/mL) was mixed with 1 mL of 0.4 mM XTT. The mixtures were incubated in dark for 2 h - 6 h under shaking. Afterwards, the mixture was filtered through a 0.2 μm surfactant-free cellulose acetate membrane filter (Thermo Scientific Nalgene Syringe Filter) to remove the MoS_2 materials. Filtered solution (250 μL) was then placed in a 96-well plate. The change in absorbance at 470 nm was monitored on a microplate spectrophotometer (MTP-880, Corona Electric Co. Ltd. Japan). TiO_2 nanoparticle (40 μg/mL) dispersion was exposed to a UV light source as a positive control.

2. Glutathione (γ-L-glutamyl-L-cysteinyl-glycine, GSH) oxidation examination by Ellman's assay

Dispersion (225 μL) of MoS_2 materials with concentrations of 20 μg/mL, 40 μg/mL or 80

μg/mL in 50 mM bicarbonate buffer (pH 8.6) was added into 225 μL of GSH (0.8 mM in the bicarbonate buffer) to initiate oxidation in microcentrifuge tube. The mixture of MoS_2 materials with GSH in the tube was covered with alumina foil to prevent illumination of light, and then placed in a shaker with a speed of 150 rpm at room temperature for incubation of 2 h, 4 h, or 6 h. After the incubation, 785 μL of 0.05 M Tris-HCl and 15 μL of 100 mM DNTB (Ellman's reagent, 5,5'-dithio-*bis*-(2-nitrobenzoic acid) (DTNB, Invitrogen or Sigma-Aldrich) were added into the mixture. MoS_2 materials were removed from the mixture by filtration through a 0.2 μm surfactant-free cellulose acetate membrane filter (Thermo Scientific Nalgene Syringe Filter). A 250 μL aliquot of the filtered solution was then placed in a 96-well plate. Their absorbance at 412 nm was measured on a microplate spectrophotometer (MTP-880, Corona Electric Co. Ltd. Japan). GSH solution without MoS_2 materials was used as a negative control. GSH (0.4 mM) oxidation by H_2O_2 (1 mM) was used as a positive control. The experiments were performed in triplicate.

Table S1. Raman peaks of raw MoS_2 power, ce-MoS_2 sheets, and aggregated ce-MoS_2.

						E^1_{2g}	A_{1g}	2LA (M)		$2E_{1g}$	$2E_{1g}$ (Γ)	E^1_{2g} + LA(M)	$2E^1_{2g}$				
raw MoS_2 powder (cm^{-1})	148.5	188.0		285.5		382.0	407.5	451.5		567.5		594.5	751.5	776.5			
ce-MoS_2 sheet (cm^{-1})	150.5	183.5	223.5	283.5	327.0	381.0	406.0	451.0	520.5 (Si)	566.5	573.5	593.5	748.5	778.0	784.5	813.82	1566.5	
aggregated ce-MoS_2(cm^{-1})	148.5	183.0	223.5	283.5		377.5	403.0	445.5		563.5	583.5	616.5	746.0	777.5		814.0	1350.5	1384.5

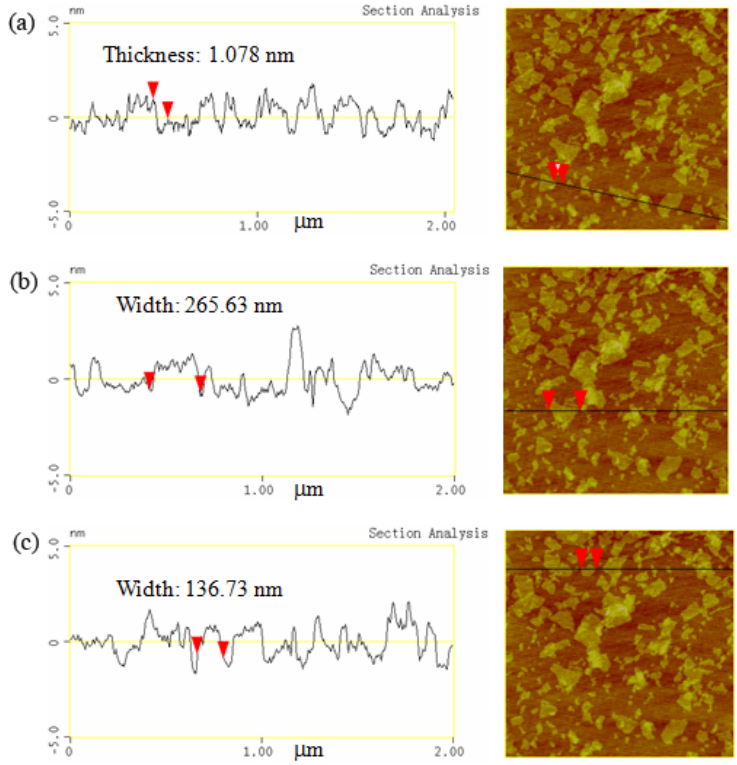

Figure S1. **AFM characterization of ce-MoS_2 sheets.** (a) A cross-sectional profile of a ce-MoS_2 sheet suggests that the ce-MoS_2 sheets are monolayers; (b) A cross-sectional profile of a ce-MoS_2 sheet suggests that the size of the ce-MoS_2 sheet is 265.63 nm; (c) A cross-sectional profile of a ce-MoS_2 sheet suggests that the size of the ce-MoS_2 sheet is 163.73 nm.

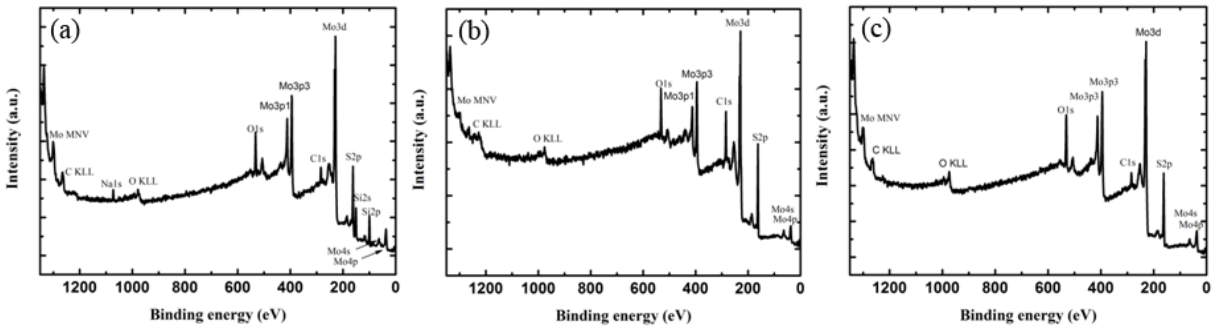

Figure S2. **XPS patterns** of (a) ce-MoS_2 sheets on Si/SiO_2 substrate; (b) Raw MoS_2 powers on Si/SiO_2 substrate; (c) Aggregated ce-MoS_2 on Si/SiO_2 substrate. The results suggest that the MoS_2 materials are highly pure.

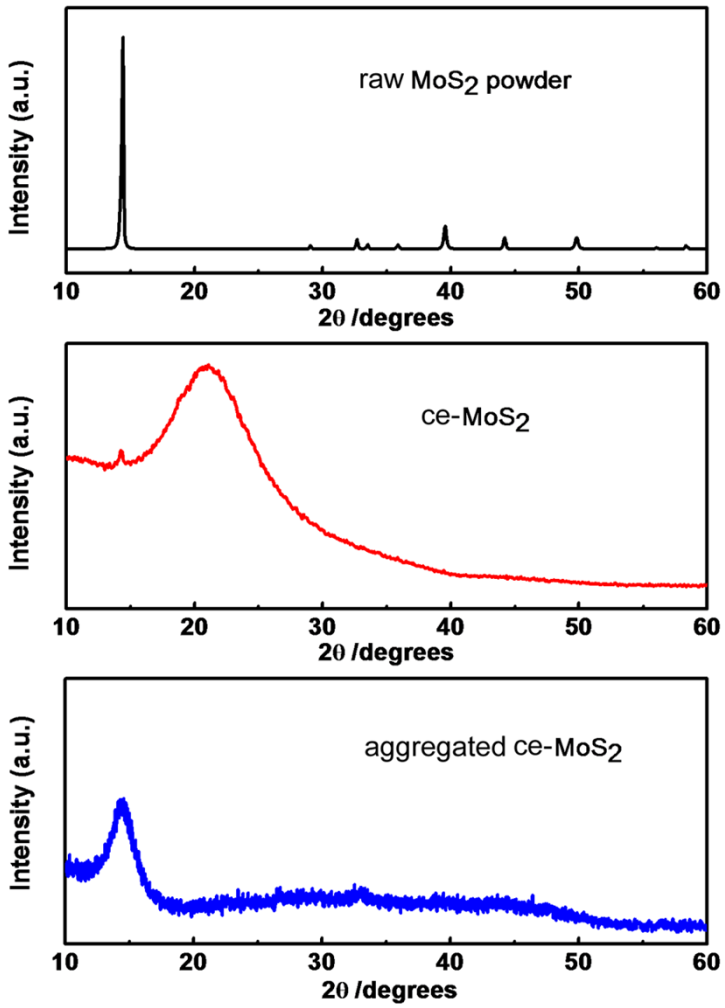

Figure S3. X-ray diffraction (XRD) spectra of raw MoS_2 powder, ce-MoS_2, and aggregated ce-MoS_2. Compared to the XRD patterns for the raw MoS_2 powder, almost all the peaks disappeared for the ce-MoS_2 sheets and the (002) peak at $2\theta=14.4^{o}$ became very weak, which is mostly due to the crystals with nanoscale sizes and the fact that the ce-MoS_2 sheets lay on the substrate with preferred orientation (Hua Zhang, et al., *Angew. Chem. Int. Ed.*, 2011, 50, 11093; Manish Chhowalla, et al., *Nano Lett.*, 2011, 11, 5111). However, the (002) peak became observable for the aggregated ce-MoS2, suggesting the monolayer MoS2 restacking together.

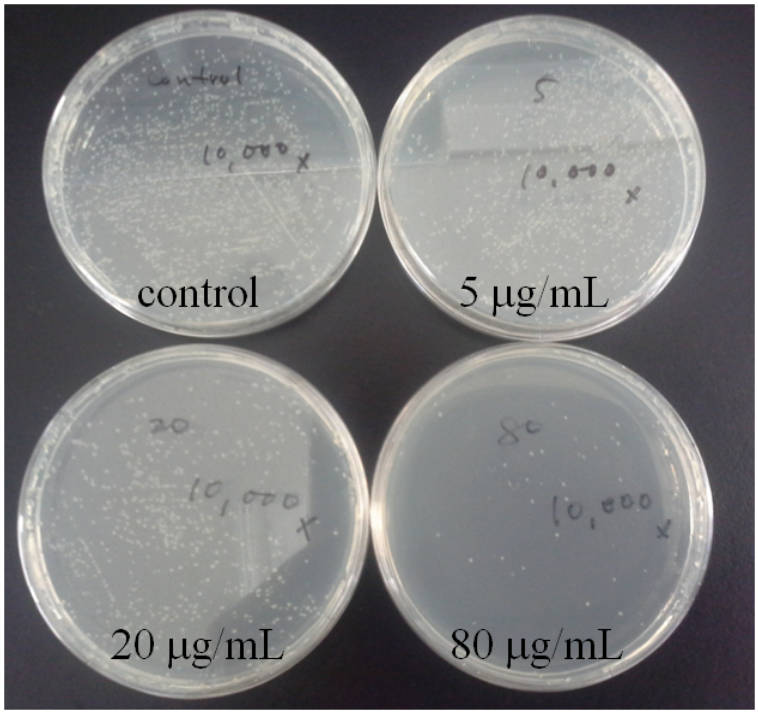

Figure S4. Digital camera photos of live *E.coli* DH5α bacteria after they were exposed to ce-MoS_2 dispersions with different concentrations for 2 h.

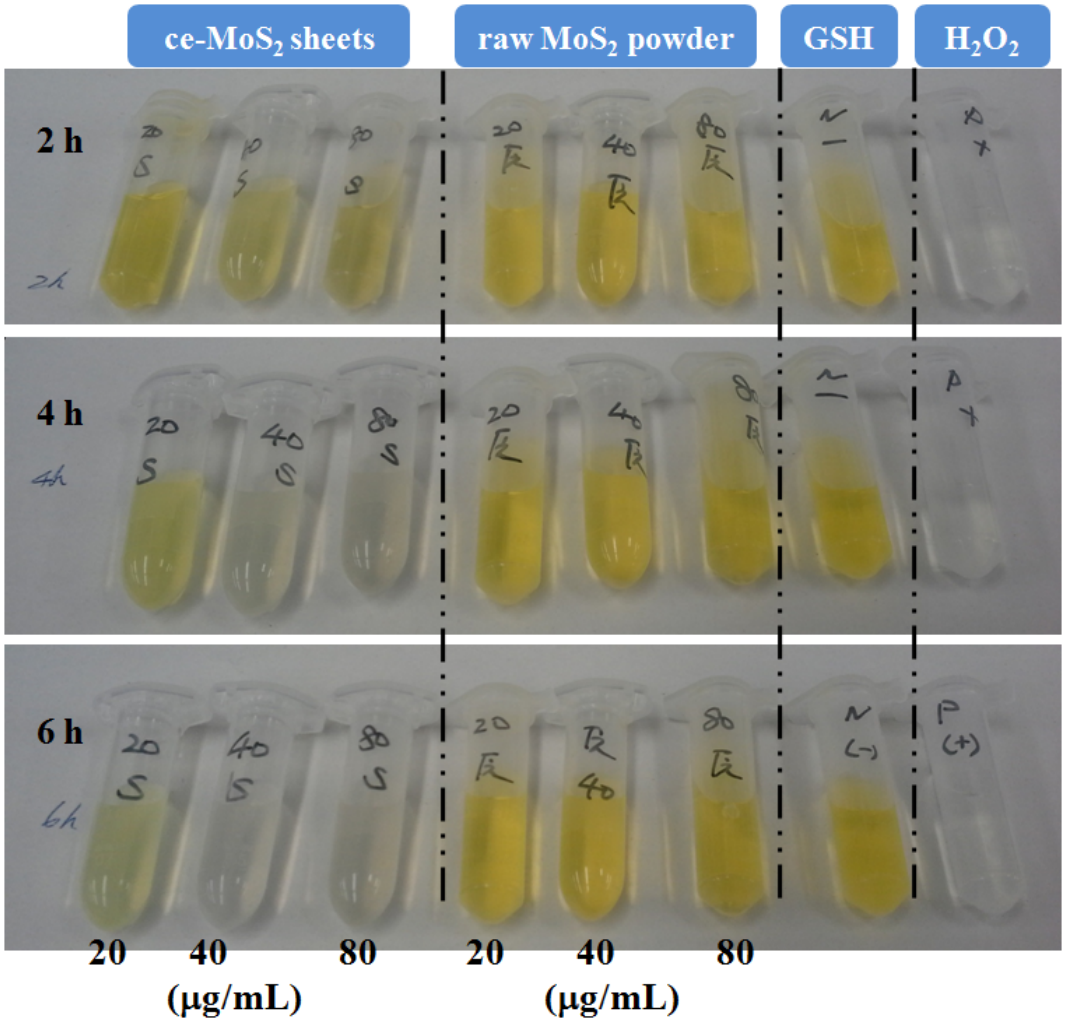

Figure S5. **Glutathione oxidation by monitoring color change.** GSH was mixed with dispersions (20, 40 or 80 μg/mL) of ce-MoS_2 sheets or raw MoS_2 powders for 2 h - 6 h. GSH solution without MoS_2 materials was used as a negative control. GSH (0.4 mM) oxidation by H_2O_2 (1 mM) was used as a positive control.

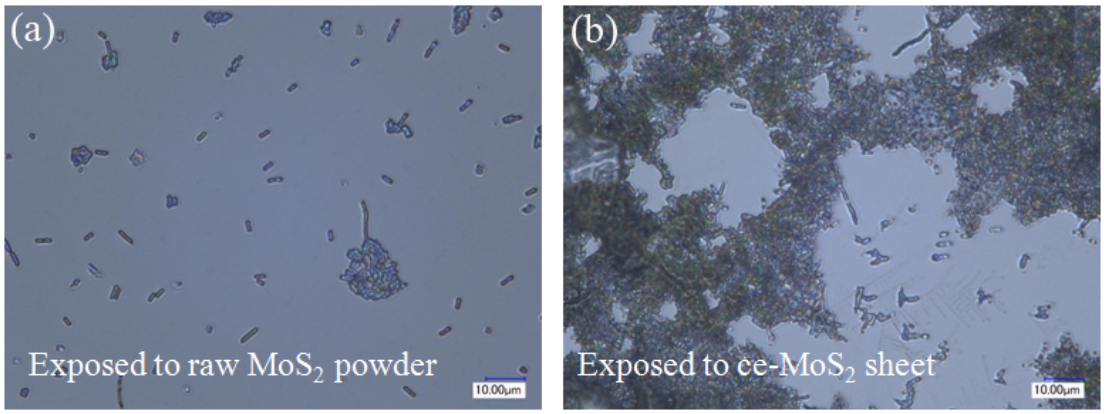

Figure S6. Keynece microscope image of the *E.coli* DH5α cells after exposure to (a) raw MoS_2 powder and (b) ce-MoS_2 sheet for 2 h. We can see after exposed to the ce-MoS_2 sheets, most the cells did not show a normal cell shape as observed on the cells exposed to the raw MoS_2 powders.

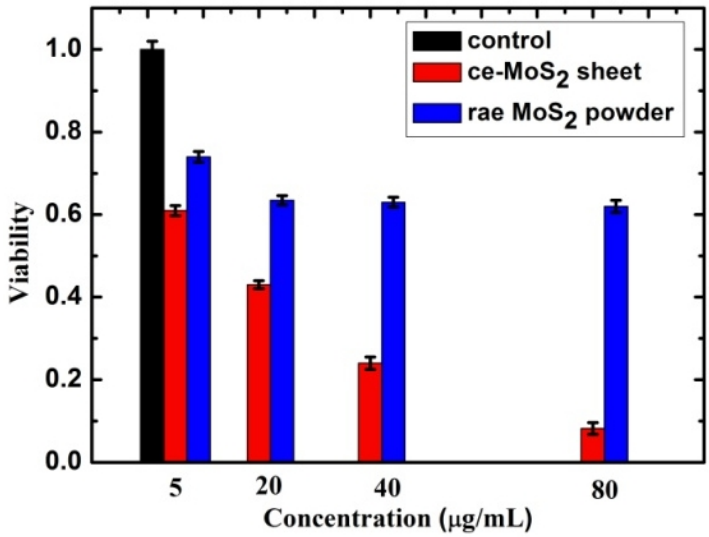

Figure S7. Concentration dependent viability of the cells after exposure of 2 h.